Dynamics in a system with time-delayed feedback

Zhao Hong,[1,2] Liu Yaowen,[1] Wang Yinghai,[1] and Hu Bambi[2,3]
[1]*Department of Physics, Lanzhou University, Lanzhou 730000, China*
[2]*Department of Physics and Centre for Nonlinear Studies, Hong Kong Baptist University, China*
[3]*Department of Physics, University of Houston, Houston, TX 77204*
(Received 7 July 1997; revised manuscript received 18 May 1998)

In this paper we study the dynamical solutions of a differential delay equation related to optical bistability. Besides the fundamental solution and the odd harmonic solution, we report different types of solutions found in moderate- and short-time delay regions, which to our knowledge, have not been discussed in earlier publications. In addition, we also study the quasiperiodic motion and the chaotic itinerancy solution of the equation. The phenomena reported in this paper are found to be the general features of delayed feedback optical systems. [S1063-651X(98)13909-0]

PACS number(s): 05.45.+b, 42.55.Px

I. INTRODUCTION

In recent years, optical feedback systems governed by differential delayed equations (DDE's) have attracted much attention from both the applied and the fundamental points of view [1–13]. Some properties of these systems have been exposed, such as the odd harmonic solutions [1–3] whose oscillation period is given by $T_F/(2k+1)$, where $k=1,2,3,\ldots$ and T_F is the period of the fundamental motion; the frequency locking and quasiperiodicity following the hierarchy of the Farey tree [4–8]; and the chaotic itinerancy phenomenon [9–11], the phenomenon that a dynamical system switches among different unstable local chaotic orbits on a time scale long compared to the dynamics on each attractor ruin. These features, however, are summarized from different systems. Questions arising from the above observations are the following. Can we meet all these phenomena in every optical system governed by DDE's? Can we find any other types of solutions in these kinds of systems?

In general, the delay-differential system related to optical bistable or hybrid optical bistable device is described by

$$\tau' \dot{x}(t) = -x(t) + f(x(t-t_R), \mu), \tag{1}$$

where $x(t)$ is the dimensionless output of the system at time t, t_R is the time delay of the feedback loop, τ' is the response time of the nonlinear medium, and the parameter μ is proportional to the intensity of the incident light. Measuring the time in units of t_R, we rewrite Eq. (1) as

$$\tau \dot{x}(t) = -x(t) + f(x(t-1), \mu), \tag{2}$$

where $\tau = \tau'/t_R$ characterizes the effect of the delay when τ' is fixed. In this paper we study Eq. (2) with the special feedback function

$$f(x,\mu) = 1 - \mu x^2. \tag{3}$$

This feedback function can be considered as the first nonlinear term of the Taylor expansion of the general nonlinear function $f(x,\mu)$ in the vicinity of a steady state. It should keep the general nonlinear properties of the delay feedback system, as pointed out by Li and Hao [12]. In the limiting case of $\tau = 0$, Eq. (2) reduces to

$$x(t) = f(x(t-1), \mu). \tag{4}$$

For the specific choice of the feedback function, Eq. (4) is just the logistic model. As the logistic model plays a crucial role in understanding the common behavior of low-dimensional dissipative nonlinear systems, we expect that Eq. (2) with the feedback function (3) may provide us with a fundamental scenario for the dynamics in systems with delayed feedback.

We organize this paper as follows. In Sec. II numerical methods used in the paper are introduced. These methods are applied to identify different types of dynamical states. In Sec. III numerical results are presented. After clarifying the fundamental solution of the system in Sec. III A, we describe different types of solutions found in the long-, moderate-, and short-time delay regions in Secs. III B, III C, and III D respectively. Section IV summarizes the main findings of the paper. In this section we also discuss to what extent the dynamical behaviors reported in the paper are the general features of the delayed feedback systems.

II. NUMERICAL METHODS

Equation (2) can only be solved numerically and a fourth-order Adam's interpolation is suitable for that. In order to trace the evolution of a DDE, one might investigate the evolution curve of the variable $x(t)$. However, it is difficult to distinguish different solutions if one only observes the $x(t)$-t relation. Some of us have described a method in Ref. [8], where we represented the solutions of a one-variable DDE by using the Poincaré section technique. This method has proved to be a useful tool in exploring the coexisting attractors. Let us review this method briefly. Let $x_t(\theta) \equiv x(t+\theta)$, $-1 \leqslant \theta \leqslant 0$; then $x_{t_2}(\theta)$ is determined by $x_{t_1}(\theta)$ uniquely according to Eq. (2), where $t_1 < t_2$. We approach the section mapping as follows. We choose an appropriate constant $x_c \in R$; integrate Eq. (2) numerically until $x(t) > x_c$ and $x(t+h) < x_c$, where h is the length of the integrating step; and then proceed with a simulation procedure or

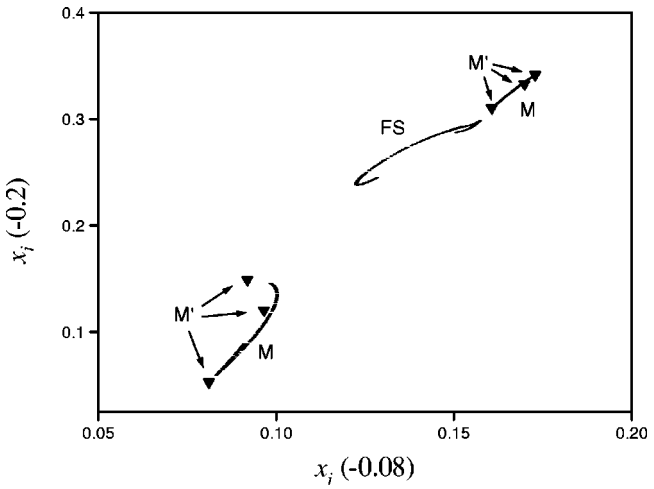

FIG. 1. Coexisting attractors at $\tau=0.81$ and $\mu=4.619$.

apply Hénon's idea [14] to get t_i as well as $x_{t_i}(\theta)$ such that $x_{t_i}(0)=x_c$. To simplify, we denote $x_{t_i}(\theta)$ as $x_i(\theta)$ in the following discussion. In this way we convert the flow of Eq. (2) into a mapping that maps the curve $x_i(\theta)$ onto the curve $x_{i+1}(\theta)$. We regard this curve-to-curve mapping as the Poincaré map of a DDE. A periodic solution of Eq. (2) with period T, $x(t)=x(t+T)$, corresponds to a periodic solution of the Poincaré map with period N, $x_i(\theta)=x_{i+N}(\theta)$, where N is an integer. For practical applications, we can take n discrete points $x_i(\theta_j)$ on the curve $x_i(\theta)$ to represent the solution, where $\theta_j\in(-1,0)$ and $j=1,2,\ldots,n$. Then the curve-to-curve mapping appears as a point-to-point mapping in R^n. In order to exhibit the coexisting attractors or show the bifurcation process, we usually need only a two-dimensional mapping representation $[x_i(\theta_1),x_i(\theta_2)]$ or a one-dimensional mapping representation $x_i(\theta_1)$. Figure 1 demonstrates a two-dimensional mapping representation of the solutions of Eq. (2) with the feedback function (3), where three coexisting attractors denoted by FS, M, and M' are shown in the $x_i(-0.08)$-$x_i(-0.2)$ plane.

After obtaining the Poincaré map, we use the definition

$$T=\lim_{i\to\infty}\frac{1}{i}\sum\ (t_{i+1}-t_i) \tag{5}$$

to characterize the oscillation period of $x(t)$. To identify different dynamical states, we usually compare the oscillation periods, see the appearances, and analyze the power spectra of them. Figure 2 shows the appearances and the corresponding power spectra of solutions in the three attractors marked in Fig. 1. T_1, T_2, and T_3 in the figure are the oscillation periods of solutions in FS, M, and M', respectively. One can find that FS and M belong to different types: The oscillation periods, the appearances, and the power spectra of solutions in them are unalike. The solutions in M and M' belong to the same type: Their oscillation periods are close to each other, their appearances are similar, and their main components in the power spectra are identical. Throughout the paper, when we mention solutions belonging to the same or different types we actually mean that they are identified to be so according to the above procedure. Finally, in order to study the bifurcation process we employ Farmer's technique [13] to calculate the Lyapunov exponents.

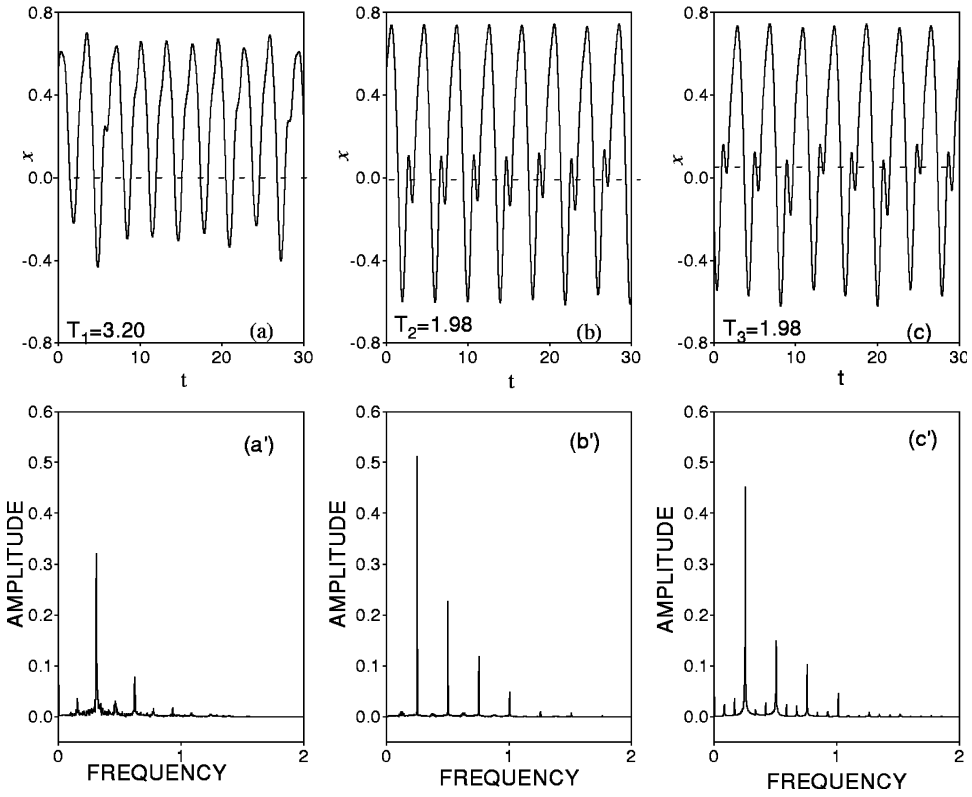

FIG. 2. Evolution curves and power spectra of the three coexisting attractors shown in Fig. 1 for (a) and (a′) FS, (b) and (b′) M, and (c) and (c′)M'.

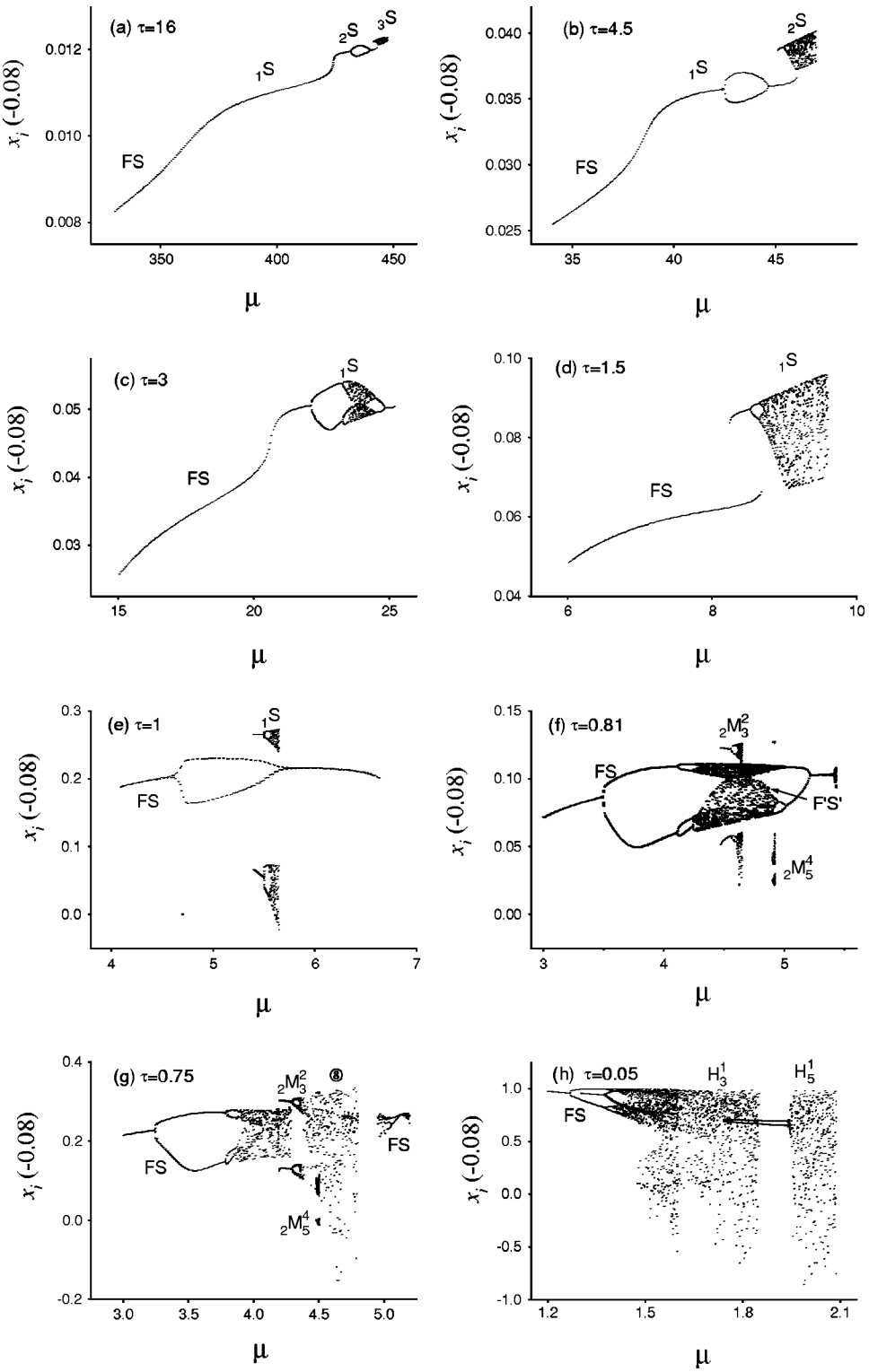

FIG. 3. Bifurcation phenomena of the system. FS, the fundamental solution; ${}_kS$, the short-time delay solutions; ${}_kM_n^m$, the moderate-time delay solutions; H_n^1, the harmonic solutions. See the text for more details.

III. RESULTS

A. Fundamental solution of the system

Equations (2) and (4) have the same steady states $x_\pm = (-1 \pm \sqrt{1+4\mu})/2\mu$ in the specific choice of the feedback function (3). These two steady states are created at $\mu = -1/4$ through tangential bifurcation. It is found that x_+ is stable in the regime of $-1/4 < \mu < \mu_0(\tau)$ while x_- is always unstable in the case of $\tau > 0$. We call the parameter regime in which x_+ is stable ''steady state'' regime in this paper.

At $\mu = \mu_0(\tau)$, the steady state x_+ bifurcates into a limit cycle through the Hopf bifurcation. The limit cycle appears as a period-1 solution of the Poincaré map of Eq. (2); therefore, we call it the period-1 periodic solution of the system. Figure 3 shows the bifurcation diagram [which is represented by $x_i(-0.08) - \mu$] originating from the period-1 periodic so-

lution, which is denoted by FS. The solutions in FS appear as square waves with oscillation period 2 when τ approaches zero. They are the analogs of the fundamental solution of the model (4). Therefore, we regard FS as the fundamental solution of the system.

Numerical calculations indicate that there exist many separated attractors besides FS in the parameter plane. In Fig. 3 we show some of them. These solutions can be classified into different classes. Solutions in the first class, e.g., the $F'S'$ marked in Fig. 3(f), possess approximate oscillation periods, similar appearances, and power spectra to those analogous of FS. In fact, tracking them on the parameter plane with the decrease of τ, we find that they must merge into FS at a certain value of τ, i.e., they turn to the periodic windows of FS. Therefore, this class of coexisting attractor should be included in the category of the fundamental solution. The other three classes of solutions are indeed specific solutions in the long-time delay region (the solutions denoted by H_n^1, with n an odd integer), moderate-time delay region (the solutions denoted by ${}_kM_n^m$, with k, m, n and integers), and short-time delay region (the solutions denoted by ${}_kS$, with k an integer). These solutions will be discussed in detail in the following subsections.

In the present subsection we describe the bifurcation process of the fundamental solution only. In the regime that τ is very large or, identically, the delay time t_R is very short, FS shows no bifurcation. It is connected with a periodic solution of another dynamical state ${}_1S$ [see Figs. 3(a)–3(c)]. With the decrease of τ, FS begins to disconnect from ${}_1S$ at $\tau=2.9$. Below this value, FS and ${}_1S$ coexist in a certain parameter region; see Figs. 3(d)–3(g). (In the region of $\tau<1$, ${}_1S$ is marked by ${}_2M_3^2$, which will be explained in Sec. III D.) At $\tau=1.13$, FS undergoes the first period-doubling bifurcation. Figure 3(e) shows a bifurcation diagram just below this value. When decreasing τ continuously, period-doubling bifurcations with higher and higher order take place until chaotic solutions appear at $\tau=0.84$. FS exhibits similar bifurcation behavior, as shown in Fig. 3(f), in the region of $0.84>\tau>0.76$. In the region of $\tau<0.76$ the bifurcation diagram of FS is divided into two parts by an embedded escaping region; see Fig. 3(g). The right-hand part disappears at $\tau=0.64$ and the left-hand part survives until $\tau=0$.

Finally, for the convenience of later discussion, let us describe briefly the dependence of the oscillation period of the fundamental solution on the system parameters μ and τ. In the region that τ is not very large the oscillation period increases as $T\sim 2+3\tau/2$ with the increase of τ. Thus oscillation periods of solutions belonging to the fundamental solution will approach 2 when $\tau\to 0$. On the other hand, the dependence of the oscillation period on the parameter μ is insensitive. For example, at $\tau=0.8$, $\Delta T/\Delta\mu\approx 0.1$; at $\tau=0.3$, $\Delta T/\Delta\mu\approx 0.02$; and at $\tau=0.1$, $\Delta T/\Delta\mu\approx 0.002$.

B. Odd harmonics: Particular solutions in long-time delay case

From Fig. 3(h) we see that there exist other solutions except the fundamental solution in the long-time delay case. Figure 4 shows several domains of the stable regions of them in the parameter plane. Numerical calculations indicate that the oscillation period of the solutions in these domains is very close to $T_F/(2k+1)$, where T_F is the oscillation period

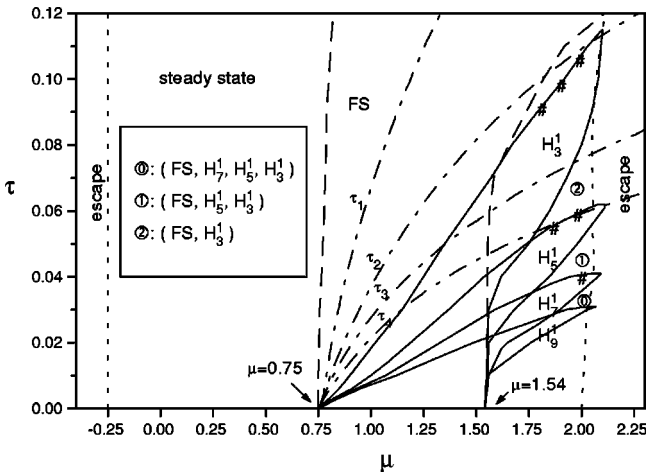

FIG. 4. Domains of the different dynamical states in the long-time delay region. Dot-dashed lines, boundaries of the escaping and bounded solution regimes; dashed lines, boundaries of the fundamental solution; solid lines, boundaries of the haramonic solutions. # denotes the regime where quasiperiodic solutions can be found. The circle-enclosed numbers mark the chaotic itinerancy regimes.

of the fundamental solution at the same value of τ and $k=1,2,3,\ldots$. Thus they are just the odd harmonic solutions of the system. The odd harmonic solution has been found to be a general feature of the delayed feedback optical systems [1–3]. In this paper we use the notation H_{2k+1}^1 to characterize the harmonic solution, i.e., the capital letter H represents the ''harmonic solution'' while the superscript and the subscript indicate the ratio of the oscillation period of the harmonic solution to that of the fundamental solution.

In fact, we can show that the odd harmonic motion is the particular behavior of the system in the long-time delay case. Let $x(t)$ be a period-1 solution of the fundamental solution at (τ,μ) and $T_F(\tau)$ denote its period. Since $x(t-kT_F)=x(t)$ (k is any integer), $x(t)$ satisfies $\tau\dot{x}(t)=-x(t)+f(x(t-1-kT_F),\mu)$. By measuring the time t with $1+kT_F$, one can rewrite this equation as $\tau_k\dot{x}(t)=-x(t)+f(x(t-1),\mu)$, where $\tau_k=\tau/(1+kT_F)$. This means that $x(t)$ is also a period-1 solution of Eq. (2) with period

$$T(\tau_k)=T_F(\tau)/[1+kT_F(\tau)] \tag{6}$$

at $\tau_k=\tau/[1+kT_F(\tau)]$. Let $T_F(\tau_k)$ be the oscillation period of the period-1 solution of the fundamental solution at (τ_k,μ). In the region that τ is close to zero, we have $T_F(\tau)\simeq T_F(\tau_k)\simeq 2$, as has been pointed out in Sec. III A, and therefore we get $T(\tau_k)=T_F(\tau_k)/(1+2k)$. From this one can immediately recognize that $x(t)$ is just the old harmonic solution at (τ_k,μ) and one can conclude that the parameter regimes of the harmonic solutions are determined by that of the fundamental solution.

We have already known that the period-1 solution of the fundamental solution exists below the curve $\tau_0=\tau_0(\mu)$, where $\tau_0(\mu)$ is the Hopf bifurcation value of the steady state x_+. Then the $(2k+1)$th harmonic solution can exist only in the regime below the curve

$$\tau_k(\mu)=\tau_0(\mu)/(1+kT_F). \tag{7}$$

Since $1+kT_F \gg 1$, harmonic solutions must exist in the region of small τ. In Fig. 4 we have plotted the curves of $\tau_k(\mu)$ with $k=1,2,3,4$ calculated according to Eq. (7) using the data $\tau_0(\mu)$ and $T_F(\tau_0,\mu)$. These curves start at the same point $(\tau,\mu)=(0,0.75)$ and then disperse each other with the increase of τ. In the region $0.75<\mu<2.2$ they are limited in the regime $\tau<0.2$ and in the region $\mu>2.2$ they fall into the escaping regime. Thus stable odd harmonic solutions of Eq. (2) with the feedback function (3) can only be observed in the regime $\tau<0.2$. From Fig. 4 one may notice that the curve $\tau_k(\mu)$ does not coincide with the left-hand boundary of the $(2k+1)$th harmonic domain. This is merely because the former is the boundary for existence while the latter is for the stable solution.

An interesting phenomenon exposed in Fig. 4 is that the left-hand and the right-hand boundaries of the harmonic domains (including that of FS) accumulate to two points, $\mu=0.75$ and $\mu=1.54$, respectively, when $\tau\to 0$. The accumulated point $\mu=0.75$ can be simply explained as the left-hand stable boundaries of harmonic domains will approach the existence boundaries when τ approaches zero. The existence of the accumulated point $\mu=1.54$ can be understood in relation to the harmonic solutions of Eq. (4) in the following way. From the well-known bifurcation diagram of the logistic map, we find that the value of $\mu=1.54$ is just the value where the two-piece strange attractor merges into a one-piece strange attractor. The images of an initial point appear at the top and bottom parts divided by x_+ alternatively in the case of a two-piece strange attractor, while the visit may become chaotic in the case of a one-piece strange attractor. We can indeed show that the point $\mu=1.54$ is also a crisis point for the harmonic solutions of Eq. (4). As a model of Eq. (2) in the limit of $\tau=0$, Eq. (4) describes the evolution of a set of initial values in a unit interval, say, $[-1,0)$. When one sets all the values in the interval equal to x_+, the evolution of Eq. (4) gives the steady state $x(t)=x_+$. Let x_1 and x_2 be the period-2 solution of the logistic map and set all the values in the interval equal to x_1; then one gets $x(t)=x_1$ for $t\in(2n-1,2n)$ and $x(t)=x_2$ for $t\in(2n,2n+1)$, where $n=0,1,2,\ldots$. This solution is the period-1 solution of Eq. (4) with oscillation period 2, by the definition of the Poincaré section. It is the analog of the period-1 solution of Eq. (2). This solution and its bifurcations contribute the fundamental solution of Eq. (4) and correspond to the fundamental solution of Eq. (2). Dividing $[-1,0]$ into $2k+1$ subintervals and putting x_1 and x_2 into them alternatively, one gets a solution $x(t)=x_1$ for $t\in(2n-2k-1,2n-2k)/(2k+1)$ and $x(t)=x_2$ for $t\in(2n-2k,2n-2k+1)/(2k+1)$, where $n=0,1,2,\ldots$ and $k=1,2,3,\ldots$. This solution is a period-1 solution of Eq. (4) too, but with the oscillation period $2/(1+2k)$. This solution and its bifurcations are responsible for the $(2k+1)$th harmonic solution of Eq. (4). In the case of $\mu<1.54$, when one applies Eq. (4) to the initial values in a subinterval, the length of the images should always remain unchanged since every image is limited in a definite part, either in the top part or in the bottom one divided by $x(t)=x_c$. This is true even for a chaotic solution. Therefore, the oscillation period of a solution remains unchanged when $\mu<1.54$. When μ exceeds this value, two or more continuous images may fall into the same part and an image may be split into some subsegments distributed in different parts. In this situation the oscillation period changes with the evolution of time continuously due to the recombination of the images, which means that solutions with definite oscillation periods must end at the point $\mu=1.54$.

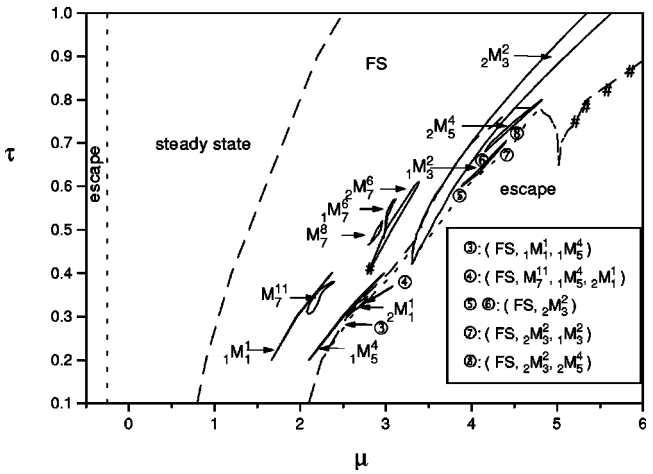

FIG. 5. Coexisting attractor domains in the moderate-time delay region. Solid-line enclosed regimes are coexisting attractor domains. The meanings of the other types of lines and symbols are the same as in Fig. 4.

Contrary to the fundamental solution, the common type of bifurcation in the harmonic domains is the so-called cascade-like bifurcation, i.e., the bifurcation after which a number of multistable periodic solutions appear simultaneously. This kind of bifurcation has been discussed and explained by Ikeda and Matsumoto [3]. Hopf bifurcations can also be seen constantly in the harmonic domains, indicating the existence of the quasiperiodic solutions for Eq. (2). Quasiperiodic solution regimes are marked by number signs in Fig. 4.

In the regimes where two or more unstable attractors exist, chaotic itinerancy among these unstable attractors may be observed. The regimes for chaotic itinerancy solutions are designated by the circle-enclosed numbers in Fig. 4. The denotation $(X,Y,Z,\ldots)$ indicates that the trajectory may switch among the unstable attractors labeled by $X,Y,Z,\ldots$, where $X,Y,Z,\ldots$ represent the harmonic components H^1_{2k+1} and the fundamental solution FS.

C. Coexisting attractors in moderate-time delay region

We have seen in Figs. 3(f) and 3(g) that there are other coexisting attractors, such as ${}_2M^2_3$ and ${}_2M^4_5$. In fact, we find many attractors coexisting with the fundamental solution in the moderate-time delay region. Figure 5 depicts ten domains of them (denoted by ${}_kM^m_n$, where n,m, and k are integers). These domains are mainly located in the region $0.2<\tau<0.9$, except the domain ${}_2M^2_3$, which extends into the regime $\tau>1$. Figure 6 shows the $x(t)-t$ diagrams of solutions in several domains in the moderate-time delay region. In this figure we also plot the evolution curves of $x(t)$ in FS and H^1_3, respectively. From the appearances of the evolution curves in these domains, together with the values of the corresponding oscillation periods printed in the figure, one can conclude that they are solutions different from the fundamental solution and the odd harmonics. It is found numeri-

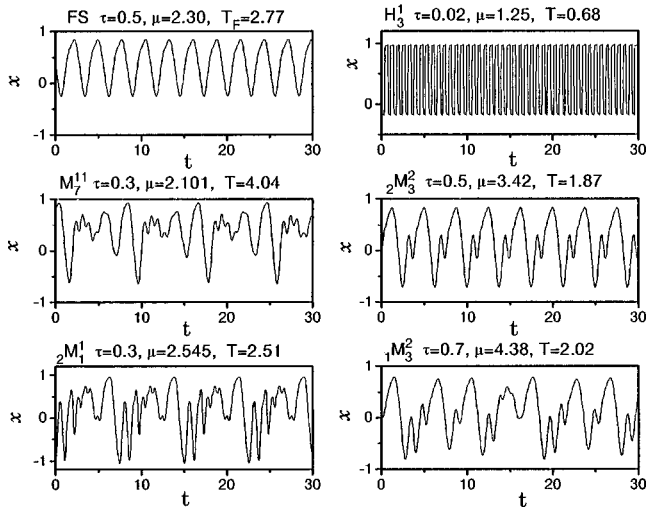

FIG. 6. Typical evolution curves in some of the coexisting attractor domains in the moderate-time delay region. For reference, the evolution curves of the fundamental solution and the third harmonic solution are also plotted.

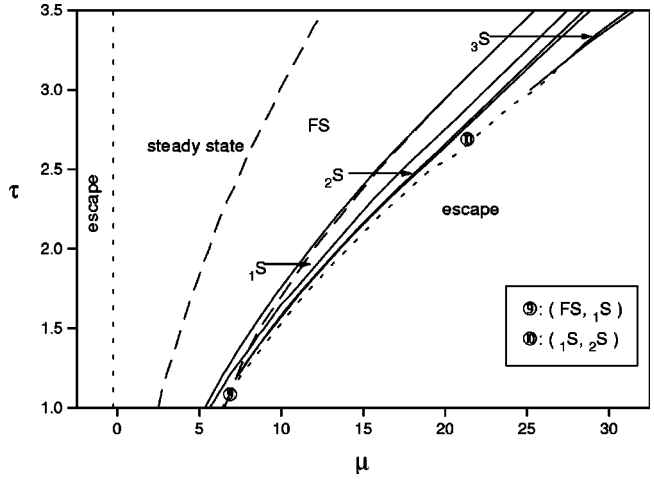

FIG. 7. Dynamics in the short-time delay region. Solid lines are the corresponding boundaries of the attractors appearing in this region. The meanings of other types of lines and symbols are the same as in Fig. 4.

cally that the ratio of the oscillation period T of solutions in a domain to the oscillation period T_F in FS is usually close to m/n, where m is an integer and n is an odd integer. Therefore, we use the notation ${}_kM_n^m$ to characterize this class of solution, where the capital letter M is used to indicate that the solutions belong to the class of the moderate-time delay region and the integers m and n give the ratio of T/T_F. Additionally, solutions in two or more different domains may have the same ratio of T/T_F; we therefore use another subscript k to distinguish them.

At a fixed τ, the oscillation period T of solutions in the interval of a domain along μ can be taken as a constant since the interval is usually very narrow (see Fig. 5) and therefore the difference of T along μ can be ignored. The oscillation period T_F of the fundamental solution may change independently of μ, as we have shown in Sec. III A. In order to obtain a definite ratio of T/T_F at a fixed τ we calculate T_F at $\mu(\tau)=\overline{\mu}(\tau)$, where $\overline{\mu}$ is the value at which the period-1 solution in FS is superstable (i.e., with the smallest value of the first Lyapunov exponent). The ratio of T/T_F for a coexisting attractor domain may change with τ, but the change is indistinguishable as long as τ is not too big. Table I shows T/T_F for ${}_2M_3^2$ and ${}_1M_1^1$ via the parameter τ, respectively. One can see that the value for the former is very close to 2/3 while for the latter it is close to 1/1 and the difference along τ can be ignored in the listed parameter region.

The most available type of bifurcation in these domains is the period-doubling one, while Hopf bifurcations are also observable. In Fig. 5 we denote a quasiperiodic solution regime induced from the Hopf bifurcation in the domain of ${}_2M_7^6$. Many chaotic itinerancy solution regimes are found in the moderate-time delay region. We also show some of them in Fig. 5.

D. Dynamics in short-time delay region

A general belief is that there is no complex phenomenon in the short-time delay region since Eq. (2) will approach a normal one-dimensional ordinary differential equation. The results in this subsection remind us that this is not the truth.

With the increase of τ, a set of new attractors appears continuously. It seems that the m/n law for T/T_F is broken in this region. So we denote simply the domains of these attractors by ${}_kS$, where $k=1,2,3,\ldots$ and the capital letter S indicates the characteristic of the short-time delay. Figure 7 shows the domains of different attractors found in the region $1<\tau<3.5$.

We have described the bifurcation process in FS in Sec. III A. Surprisingly, the bifurcation process observed in every domain in the short-time delay region is strikingly similar to that in FS. This can be found easily when one returns to Fig. 3 and compares the bifurcation processes of ${}_1S$, ${}_2S$, ${}_3S$, and FS with each other. Here we just want to describe some details in the adjacent regimes of two domains. In the case of Figs. 3(a)–3(c), FS shows only a period-1 solution and it is connected with that of ${}_1S$ in the bifurcation diagram. In this regime, it is difficult to determine the exact boundary of ${}_1S$ and FS. Actually, the $x(t)$-t curve in ${}_1S$ seems more similar

TABLE I. T/T_F of ${}_2M_3^2$ and ${}_1M_1^1$ via τ.

τ	$\overline{\mu}$	T_F	$\mu({}_2M_3^2)$	$T({}_2M_3^2)$	$T({}_2M_3^2)/T_F$	τ	$\overline{\mu}$	T_F	$\mu({}_1M_1^1)$	$T({}_1M_1^1)$	$T({}_1M_1^1)/T_F$
0.9	2.9	3.08	4.92	2.00	0.65	0.4	1.5	2.65	2.37	2.67	1.01
0.8	2.6	3.01	4.42	1.97	0.65	0.35	1.4	2.58	2.195	2.60	1.01
0.7	2.3	2.94	4.10	1.95	0.66	0.3	1.4	2.52	1.958	2.50	0.99
0.6	2.0	2.86	3.65	1.90	0.66	0.25	1.3	2.44	1.85	2.42	0.99
0.5	1.8	2.76	3.40	1.87	0.67	0.2	1.2	2.36	1.6645	2.34	0.99

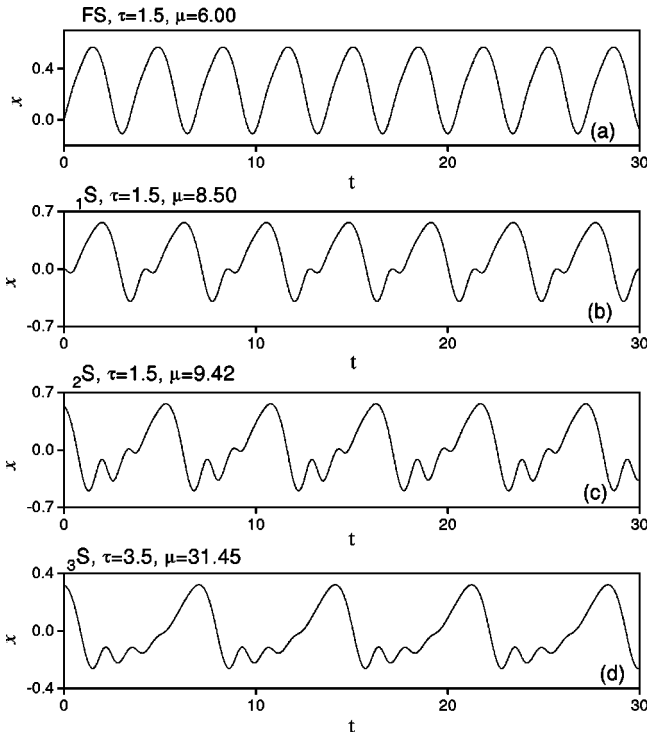

FIG. 8. Evolution curves of solutions in (a) FS, (b) $_1S$, (c) $_2S$, and (d) $_3S$.

to that in FS. In this situation we divide the two domains only by observing the bifurcation diagram, i.e., we take the value of μ where an obvious change on the bifurcation diagram can be seen as the boundary of the two domains. When we decrease τ to $\tau=2.9$, FS and $_1S$ begin to disconnect from each other in the bifurcation diagram. The bifurcation diagram in the adjacent region exhibits a typical bistability when $\tau<2.9$; see Fig. 3(d). Again, this picture is suitable for the adjacent regimes of $_1S$ and $_2S$, $_2S$ and $_3S$, etc. On the other hand, though the appearance of the $x(t)$-t curves in these domains are different, from Fig. 8 one can find similarities between them: The solution in FS has only one peak within one period, the solution in $_1S$ has another small peak, and the solutions in $_2S$ and $_3S$ have more and more peaks with smaller and smaller amplitude. We have investigated the region until $\tau=100$ and found that the similarities remain for all the continuously appearing attractors.

From Fig. 3 one can find that the scale of the bifurcation diagrams of $_kS$ increases along the horizontal direction and decreases along the vertical direction with the increase of k. We have compared the bifurcation diagrams of $_kS$ with each other at their critical values of τ_k, where τ_k is chosen to be the value below which the second period-doubling bifurcation of the period-1 periodic solution in $_kS$ will take place. Our calculations show that τ_k increases exponentially when k increases. For each value of τ_k we measured the length of $\delta\mu(_kS)$ of the period-2 periodic solution in the direction of μ and use it to characterize the scale of $_kS$ along the horizontal direction. According to our numerical results, the scale of $_kS$ increases exponentially along the horizontal direction and decreases exponentially in the vertical direction.

From Fig. 7 we see that the domains of $_kS$ all end before $\tau<1$ except the domain of $_1S$. The $_1S$ domain is extended

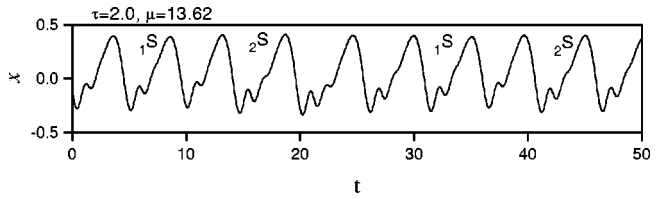

FIG. 9. Chaotic itinerancy between $_1S$ and $_2S$.

into the moderate-time delay region and disappears at $\tau\sim0.42$. In the moderate-time delay region the ratio of the oscillation period of solutions in this domain to that in the fundamental solution approaches a rational fraction ($T/T_F=2/3$), which is a common characteristic of the solutions in the moderate-time delay region. Thus we include the part of the domain in the region of $\tau<1$ in the class discussed in Sec. III C and mark this part as $_2M_3^2$.

Chaotic itinerancy solutions can be observed in relatively large regimes in this region (see Figure 7). Fig. 9 shows a chaotic itinerancy solution found in the regime denoted by the circle-enclosed 10.

IV. CONCLUSIONS

In conclusion, we investigated in detail a DDE with a simple nonlinear feedback function in the parameter plane and explored a more general scenario of the dynamical behaviors in the delayed feedback optical systems. In the case of long-time delay we observed the odd harmonic solutions whose behaviors agree with the scenario of Ikeda and coworkers [2,3]. We explained why this kind of solution can only be observed in the long-time delay case. In addition, we found that the left-hand boundaries and the right-hand boundaries of the stable odd harmonics domains as well as FS in the parameter plane accumulate at two points, respectively, when τ tends to zero. In the case of moderate-time delay, we found a set of attractors with oscillation periods approaching mT_F/n, where m is an integer, n is an odd integer, and T_F is the oscillation period of the fundamental solution. When we investigated the short-time delay region, we recognized that there exists another family of stable solutions. The solutions in this family have similar bifurcation processes and appearances. The existence of these solutions indicates that one can find chaotic solutions even when the delay time is very short, provide the parameter μ is large enough. The fundamental solution and the odd harmonics of the DDE have analogs in Eq. (4), i.e., the model of the system (2) in the limiting case of $\tau=0$. The two classes of the solutions found in the moderate- and short-time delay cases have no counterparts in the model of $\tau=0$. We would like to point out that, to our knowledge, these two classes of solutions have not been reported in previous studies related to delayed feedback systems. Besides the types of solutions mentioned above, our results also show that the chaotic itinerancy phenomenon and quasiperiodic motion can be observed in a wide region in the parameter plane of the DDE.

Finally, we would like to emphasize that the dynamics described in this paper is a general feature of the delayed feedback optical systems. As pointed out in the Introduction, the feedback function used in the present paper can be considered as the first nonlinear term of the Taylor expansion of

a general nonlinear function in the vicinity of a steady state and therefore one can expect that it should keep the general properties of these kinds of delay feedback systems. In fact, we have studied Eq. (2) with $f(x,\mu)=\pi\mu[1+2B\cos(x-x_0)]$, the model Ikeda and co-workers; $f(x,\mu)=\pi[A-\mu\sin^2(x-x_0)]$, the Vallée model; $f(x,\mu)=\mu\sin^2(x-x_0)$, the sine-square model; and other nonlinear functions. The global behaviors related to the delay time, i.e., the fundamental solution, the harmonic solution, and new types of solutions observed in the moderate- and the short-time delay regions, can all be found with the variation of the delay time. The details are more complex than the case of the logistic form. On the one hand, the structure of the bifurcation diagram for a specific attractor, i.e., the structure of the periodic windows, is determined by the function f and is similar to the bifurcation diagram of the model in $\tau=0$. On the other hand, nonlinear functions other than the logistic form may have more than one stable steady state. These states may induce fundamental solutions and other types of solutions mentioned above independently and the induced solutions may merge into large attractors in certain parameter regimes.

ACKNOWLEDGMENTS

We acknowledge fruitful discussions with Professor B. L. Hao, Professor Y. Gu, and Dr. Z. G. Zheng. This work was supported in part by the Natural Science Foundation of China, Hong Kong Research Grant Council Grant No. RGC/96-97/10 and the Hong Kong Baptist University Faculty Research Grants Nos. FRG/95-96/II-09 and FRG/95-96/II-92.

[1] F. A. Hopf, D. L. Kaplan, H. M. Gibbs, and R. L. Shoemaker, Phys. Rev. A **25**, 2172 (1982).
[2] K. Ikeda, K. Kondo, and O. Akimoto, Phys. Rev. Lett. **49**, 1467 (1982).
[3] K. Ikeda and K. Matsumoto, Physica D **29**, 223 (1987).
[4] D. Baums, W. Elsäßer, and E. O. Göbel, Phys. Rev. Lett. **63**, 155 (1989).
[5] J. Mørk, J. Mark, and B. Tromborg, Phys. Rev. Lett. **65**, 1999 (1990).
[6] J. Sacher, D. Baums, P. Panknin, and E. O. Göbel, Phys. Rev. A **45**, 1893 (1992).
[7] J. Ye, H. Li, and J. G. McInerney, Phys. Rev. A **47**, 2249 (1993).
[8] H. Zhao, F. Z. Zhang, J. Yan, and Y. H. Wang, Phys. Rev. E **54**, 6925 (1996).
[9] K. Otsuka, Phys. Rev. Lett. **65**, 329 (1990).
[10] I. Fischer, O. Hess, W. Elsäßer, and E. Göbel, Phys. Rev. Lett. **73**, 2188 (1994).
[11] C. Masoller, Phys. Rev. A **50**, 2569 (1994).
[12] J. N. Li and B. L. Hao, Commun. Theor. Phys. **11**, 265 (1989).
[13] J. D. Farmer, Physica D **4**, 366 (1982).
[14] M. Hénon, Physica D **5**, 412 (1982).